THERMAL ENVIRONMENT IMPROVEMENT AND PARAMETER OPTIMIZATION OF WET CURTAIN FAN VENTILATION IN A GREENHOUSE: A CFD STUDY WITH EXPERIMENTAL VALIDATION

/

温室湿帘风机通风热环境改善与参数优化：CFD 研究与实验验证

Huanran SUN[1, 2], Binguang JIA[*3], Ziye SONG[4]

[1]Shandong Huayu University of Technology, Dezhou, 253023, China;

[2]Shandong Engineering Research Center of Low-Carbon Energy Internet of Things Technology, Dezhou, 253023, China;

[3]Department of Mechanical and Electrical Engineering, Jinan Engineering Polytechnic, Jinan, 250200 China;

[4]Civil and Transportation Engineering College, Weifang University, Weifang 261000, China.

Tel:13688624631; E-mail: jiabinguang78@163.com

DOI: https://doi.org/10.35633/inmateh-79-14

Keywords: *Greenhouse, Wet curtain, Temperature, Velocity*

ABSTRACT

Effective cooling is crucial for maintaining suitable thermal environments in greenhouses during hot summers. This study developed a coupled numerical model to investigate the cooling performance of a wet curtain system in a multi-span plastic greenhouse in Weifang, China. Relative deviations were less than 5.88% for wet curtain outlet temperature and below 7% for average greenhouse temperature. Results indicated that the wet curtain reduced the average greenhouse temperature by 2.33 ~ 4.20 ℃, with the maximum reduction of 4.20 ℃ occurring at 12:00. The cooling capacity increased with rising solar radiation in the morning and then diminished in the afternoon. The cooled air entered as a floor-level jet, accumulated near the crop zone, and subsequently rose due to buoyancy, forming two large recirculation vortices that enhanced vertical mixing and improved temperature uniformity. Consequently, the average indoor air velocity increased by 8.38% ~ 22.40% compared to ventilation without the wet curtain. Parametric analysis revealed that the average greenhouse temperature decreased nonlinearly with increasing inlet velocity, and the marginal cooling benefit dropped significantly when the inlet velocity exceeded 0.75 m/s. An optimal inlet velocity range of 0.75 ~ 1.0 m/s is recommended. The model accurately captured the thermal performance and airflow patterns of the greenhouse with wet curtain cooling.

摘要

在炎热的夏季，有效的降温对维持温室适宜的热环境至关重要。本研究建立了一个耦合数值模型，用于研究山东潍坊一座连栋塑料温室中湿帘系统的降温性能。湿帘出口温度的相对偏差小于 5.88%，温室平均温度的相对偏差小于 7%。结果表明，湿帘使温室平均温度降低了 2.33 ~ 4.20 ℃，其中 12:00 时降幅最大，达 4.20 ℃。上午降温能力随太阳辐射增强而提高，午后则逐渐减弱。冷却后的空气以贴地射流形式进入温室，在作物区附近积聚，随后因浮力作用上升，形成两个大型回流涡，增强了垂直混合，改善了温度均匀性。因此，与无湿帘的通风相比，室内平均风速提高了 8.38% ~ 22.40%。参数分析显示，温室平均温度随入口风速的增加呈非线性下降，当入口风速超过 0.75 m/s 时，边际降温效益显著降低。推荐的最佳入口风速范围为 0.75 ~ 1.0 m/s。该模型准确捕捉了湿帘降温温室的热工性能和气流流型。

INTRODUCTION

With the global population projected to reach 8.5 billion by 2030 (*Abedrabboh et al., 2024*), the demand for food is explosive growth, with an estimated increase of 50% (*Bergman et al., 2011*), thereby placing greater pressure on water resources and arable land. Consequently, enhancing food yield has become a critical issue in addressing food security.

Greenhouse is a facility that utilize solar energy to enable off-season crop cultivation (*Dietz et al., 2011*). Greenhouses transmit shortwave solar radiation while blocking longwave radiative loss, thus maintaining a favorable thermal environment for off-season cultivation (*Zhang et al., 2025*).

Huanran Sun, M.S. Eng.; Binguang Jia, Prof. Ph.D.; Ziye Song, Prof. Ph.D.

Compared with open-field cultivation, the greenhouse contributes to a notable increase in overall crop yield, as greenhouse can monitor and regulate growing conditions (*Garcia et al., 2026*). At the same land area, tomato production in greenhouse can achieve yields approximately 15 times higher than those obtained in open-field systems (*Abedrabboh et al., 2024*). Furthermore, off-season crop marketing can significantly elevate market prices, which contributes to enhance the economic profitability of agricultural production (*Lei et al., 2023*). Although greenhouses can maintain suitable internal conditions for the growth for horticultural products in winter, the greenhouse effect intensifies internal temperatures during summer, leading to increased pest and disease incidence and, in severe cases, dehydration and crop mortality (*Rahman et al., 2021*). Therefore, effectively providing an optimal growing environment under high-temperature summer conditions has become a prominent research focus in the horticulture (*Krishna et al., 2024*).

Based on cooling strategies, summer greenhouse cooling can be categorized into passive and active approaches (*Zhang et al., 2022*). Passive cooling relies on natural ventilation driven by indoor–outdoor temperature gradients. Although optimizing vent configurations can improve airflow and temperature distribution (*Park et al., 2022*). Some researchers (*Moreno-Teruel et al., 2022*) noted that the increase in the greenhouse width could enhance crop radiation interception and elevate internal CO_2 concentrations for the passive cooling strategy. The greenhouse designed by Yang et al. demonstrated superior performance over front roof and side vent configurations under both sunny and overcast conditions, resulting in improved crop growing environments and a 7.9% increase in tomato yield (*Yang and Liu, 2024*). Despite extensive research on passive cooling techniques, the limited temperature gradient between the interior and exterior renders passive cooling insufficient to ensure adequate crop growth conditions during summer.

Active cooling techniques employ fans to forcibly introduce outdoor air or cold air generated by mechanical cooling systems into the greenhouse (*Peng et al., 2023*). Depending on the cold source, active cooling can be divided into artificial cooling and natural cooling. Compared with natural ventilation, forced ventilation can provide the required airflow rates in summer but may still induce spatial temperature heterogeneity (*Jerszurki et al., 2021*; *Yoon et al., 2024*).

When the environment temperature was greater than the suitable temperature for crop growth in summer, wet curtain systems, which relied on the core mechanism of evaporative cooling, could produce air cooler than ambient conditions, emerging as a critical solution for summer greenhouse cooling (*Shen et al., 2026*). As wet curtain achieved temperature reductions of 5 to 15 °C while consuming only one-quarter to one-third of the energy required by conventional air conditioning, wet curtain greenhouse cooling systems have attracted considerable research interest (*Chen et al., 2023*).

However, a critical shortcoming persists in most CFD studies on wet curtain greenhouses. To simplify computation, the cooling effect of the wet curtain is typically predefined as a fixed temperature drop or a fixed cooling efficiency based on empirical correlations. Although this empirical boundary treatment is computationally efficient, it neglects the dynamic interactions among the incoming air velocity, the heat and mass transfer within the water film, and the fluctuating outdoor climatic conditions (solar radiation and air humidity). Consequently, such simplifications cannot capture the transient response of the cooling system, and under highly variable solar radiation loads, they may cause significant deviations in the predicted spatial distributions of airflow and temperature. This study proposes a mechanistic-coupling modeling approach. Unlike conventional empirical methods, the heat and mass transfer equations of the wet curtain are embedded into the greenhouse mathematical model via user-defined functions (UDFs). This integration enables the inlet boundary conditions at the wet curtain to dynamically respond to real-time outdoor environmental parameters, rather than being prescribed in advance.

MATERIALS AND METHODS

Description of experimental greenhouse

The experimental facility employed in this study was a large-scale multi-span plastic greenhouse in Weifang City, China (118°32′E, 36°41′N). As illustrated in **Fig. 1**, the greenhouse were 36 m in length, 16 m in width and 4.5 m in height. Along the longitudinal direction, the structure was divided into four identical modules, each with a length of 9 m. Each module was equipped with an air inlet and an outlet, both measuring 4 m in width and 1.5 m in height. A wet curtain pad matching the inlet dimensions was installed at the air intake, with a fan positioned downstream of the pad. The roof adopted an arched configuration, reaching a maximum height of 4.5 m, while the surrounding sidewalls, which connect to the arched roof, have a height of 3 m.

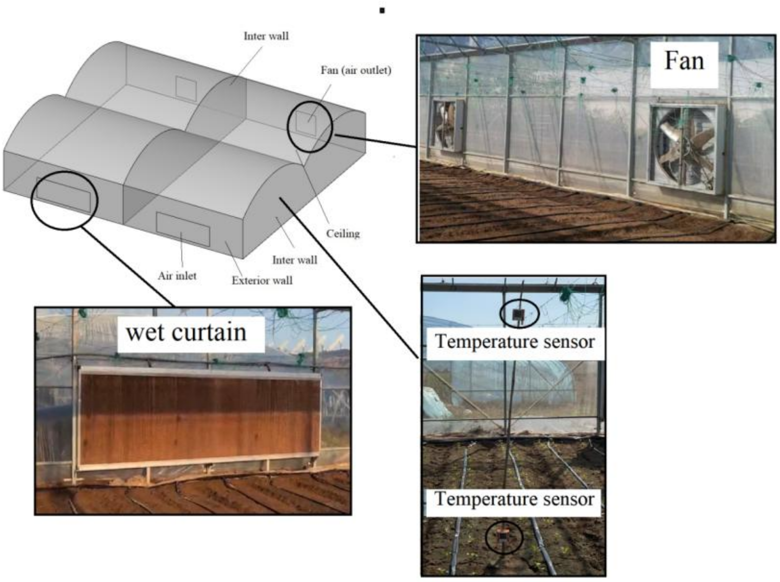

Fig. 1 - Experimental greenhouse structure and location of observation points

Cooling experiments were conducted on September 17, 2025, between 8:00 and 17:00. This date was deliberately chosen to avoid interfering with the ongoing crop production cycle, as the greenhouse is a commercial cultivation facility. Measurements were therefore scheduled during a non-planting window while the house was empty, and the day itself was a typical clear, hot day representative of the late-summer climatic conditions requiring cooling. The ambient temperature ranged from 18.8 ℃ to 28.2 ℃, and the relative humidity varied between 39.4% and 58.8%. The wet curtain pad was supplied with recirculating water maintained at a controlled temperature of 18–20 ℃. The water flow rate was set according to the pad manufacturer's specification to ensure complete wetting of the pad surface, approximately 30 L·min^{-1}. The evaporative cooling efficiency of the pad under these operating conditions is approximately 80%. A total of 10 temperature monitoring points were arranged inside the greenhouse, distributed between the upper and lower regions to capture vertical temperature variations. Temperature measurements were performed using Testo 174H data loggers (operating range: -20 ~ 70 ℃; accuracy: ±0.5 ℃). Solar radiation, which was mounted above the west side of the greenhouse roof, was recorded using a TBQ-2 pyranometer (measurement range: 0 ~ 2000 W/m; accuracy: 5 %; sensitivity: 8.963 μV·W/m²; spectral range: 0.3 ~ 3.0 μm). Ambient wind speed was monitored using a YGC-FS anemometer (measurement range: 0 ~ 45 m/s; resolution: 0.1 m/s; accuracy: ± (0.3 + 0.03 V) m/s) positioned on the western side of the greenhouse.

Physical model and mesh generation

The physical model of the greenhouse was established and meshed by Gambit software. As illustrated in **Fig. 2**, the experimental greenhouse could be divided into several geometrically identical modules; therefore, to reduce computational expense, only one module was selected for physical modeling. After the model construction, mesh generation was performed. The mesh configuration of the greenhouse was depicted in **Fig. 2**. Mesh quality assessment revealed a maximum skewness of 0.82, with 93.8% of grid elements exhibiting a skewness below 0.6, indicating satisfactory mesh quality suitable for subsequent simulations.

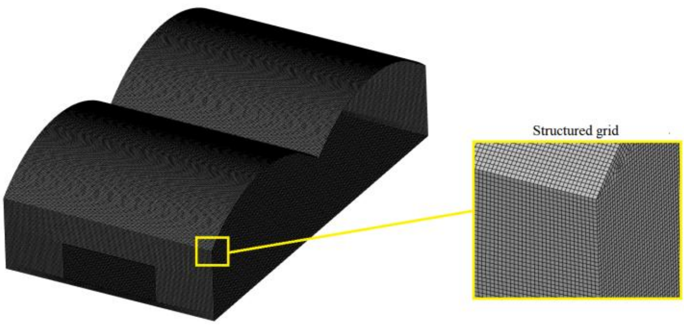

Fig. 2 – Grid generated in greenhouse computational domain

To achieve a balance between computational speed and accuracy, a grid independence test was performed using seven systematically refined meshes under conditions without wet curtain ventilation. The resulting average temperatures were plotted in **Fig. 3**. As the mesh was refined, the predicted average temperature decreased monotonically and the variation became negligible beyond 3.49 × 10^6 elements. To quantitatively assess the discretization error, the Grid Convergence Index (GCI) was calculated. GCI for the fine-grid solution was determined to be 1.36%, confirming that the discretization uncertainty is sufficiently small. Consequently, the mesh with 3.49 × 10^6 elements was selected as an appropriate compromise between accuracy and computational cost.

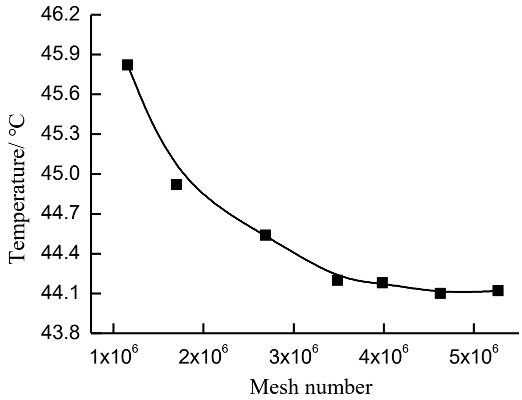

Fig. 3 - Average temperature with respect to mesh number

Governing equations

Computational fluid dynamics simulation techniques could discretize the system of partial differential equations governing fluid flow in both space and time, and obtain physical quantities (e.g., velocity, pressure, temperature) at discrete points through iterative solution of the resulting algebraic equations. This approach provided a convenient and effective means for parametric investigations of greenhouse cooling using wet curtain systems.

Prior to conducting the numerical simulations, the following assumptions were adopted (*Jiao et al., 2024*):

(1) The effects of crop respiration and transpiration on the temperature and velocity distributions of air inside the greenhouse are neglected;

(2) The Boussinesq approximation is employed to account for the influence of buoyancy forces on airflow;

(3) Infiltration of cold air into the greenhouse is disregarded.

(4) There are no crops being cultivated in the greenhouse.

The continuity, momentum, and energy equations for the air region within the greenhouse are expressed as follows (*Fu et al., 2023*):

$$\frac{\partial \rho}{\partial t}+\nabla\left(\rho \vec{v}\right)=0 \tag{1}$$

$$\frac{\partial}{\partial t}\left(\rho \vec{v}\right)+\nabla\left(\rho \vec{v}\vec{v}\right)=-\nabla P+\nabla\cdot\left(\overline{\overline{\tau}}\right)+\rho \vec{g} \tag{2}$$

$$\frac{\partial}{\partial t}(\rho E)+\nabla\cdot\left(\vec{v}(\rho E+P)\right)=\nabla\cdot\left(k_{eff}\nabla T-\sum_j h_j \vec{J}_j+\left(\overline{\overline{\tau}}_{eff}\cdot\vec{v}\right)\right) \tag{3}$$

where: ρ was the air density (kg/m³); t was time (s); v was velocity vector (m/s); P was the pressure (Pa); τ was the stress tensor (Pa); g was the gravitational acceleration vector (m/s²); E was the total energy per unit mass (J/kg); k_{eff} was the effective thermal conductivity (W/(m·K)); T was Temperature (K); h_j was the enthalpy of species (J/kg); J_j was diffusion flux of species (kg/(m²·s)); τ_{eff} was the effective stress tensor (Pa).

Given that the airflow in a greenhouse typically exhibits complex turbulent characteristics, specifically manifested as high-strain-rate flow formed when cold air jets impinge on the ground, and large-scale recirculation vortices driven by buoyancy after heating (*Allali et al. 2024*). To more accurately predict the velocity and temperature distributions inside the greenhouse, this study adopts the RNG *k-ε* turbulence model based on renormalization group theory. Compared with the standard k-ε model, the RNG *k-ε* model introduces an additional source term into the ε equation and modifies the calculation formula for turbulent viscosity, thereby enabling more effective handling of high strain rates, streamline curvature, and the nonlinear effects of buoyancy on the turbulent structure (*Chen, 2015*). This model has been widely applied in CFD simulations of greenhouse environments and similar building ventilation, and can reasonably resolve the temperature stratification and vortex structures of interest in this study.

$$\frac{\partial(\rho k)}{\partial t}+\frac{\partial(\rho k u_i)}{\partial x_i}=\frac{\partial}{\partial x_j}\left[\alpha_k \mu_{eff}\frac{\partial k}{\partial x_j}\right]+G_k+\rho\varepsilon \tag{4}$$

$$\frac{\partial(\rho\varepsilon)}{\partial t}+\frac{\partial(\rho\varepsilon u_i)}{\partial x_i}=\frac{\partial}{\partial x_j}\left[\alpha_\varepsilon \mu_{eff}\frac{\partial \varepsilon}{\partial x_j}\right]+\frac{C_{1\varepsilon}^*}{k}G_k-C_{2\varepsilon}\frac{\beta\varepsilon^2}{k} \tag{5}$$

where: G_k was the generation term of turbulent kinetic energy; k caused by the average velocity gradient; $C_{1\varepsilon}$ and $C_{2\varepsilon}$ were empirical constants; $C_{1\varepsilon}$=1.42, $C_{2\varepsilon}$ = 1.68.

The discrete ordinates (DO) radiation model implemented in the CFD framework enables the incorporation of solar radiation as a function of longitude and latitude. The DO radiation model was selected for calculating solar radiation, with the relevant governing equations provided below (*Jiao et al., 2024*).

$$\nabla\left(I_\lambda\left(\vec{r},\vec{s}\right)\vec{s}\right)+(\alpha_\lambda+\sigma_s)I_\lambda\left(\vec{r},\vec{s}\right)=\alpha_\lambda n^2\frac{\sigma T^4}{\pi}+\frac{\sigma_s}{4\pi}\int_0^{4\pi}I_\lambda\left(\vec{r},\vec{s}\right)\Phi\left(\vec{s}\cdot\vec{s}'\right)d\Omega' \tag{6}$$

The physical properties employed in the governing equations are summarized in Table 1.

Where: $\vec{r}$ was the position vector; $\vec{s}$ was the direction vector, *a* was the absorption coefficient, n was the refractive index, σs was the scattering coefficient, σ was the Stefan-Boltzmann constant (5.672×10^{-8} W·m^{-2}·K^{-4}); *I* was the radiation intensity (W·m^{-2}), Φ was the phase function, Ω' was the solid angle.

The physical properties employed in the governing equations are summarized in Table 1 (*He et al., 2018*).

Table 1

Physical property parameters in mathematical model

Name	Density/ Kg/m³	Specific heat capacity/ J/(kg·K)	Thermal conductivity/ W/(m·K)	Absorptivity	Transmittance	Viscosity/ Pa·s	Coefficient of thermal expansion/ 1/K
Air	0.91	1006.4	0.0242	0	1	1.79×10^{-5}	3.34×10^{-3}
Soil	1300	800	1.3	0.4	0	-	-
Polycarbonate	920	2300	0.4	0.3	0.7	-	-

Boundary conditions

Near-wall regions were treated using the standard wall function approach. The roof, sidewalls, and ground surface of the greenhouse were all configured as wall boundary conditions. For these boundaries, the free-stream temperature was set to the ambient temperature, and the convective heat transfer coefficient was assigned a value of 15 W/ (m²·K). At the greenhouse inlet, fans were installed to force outdoor air through the wet curtain, where it was cooled before being delivered into the greenhouse interior. A velocity inlet boundary condition was prescribed at the inlet. The corresponding inlet velocities were set as 0.25 ~ 1.50 m/s. The temperature variation of the incoming air was determined by solving the heat and mass transfer processes within the wet curtain. The outlet air temperature was calculated using the following expression (*Jiang et al., 2021*):

$$T_{wc,out}=T_{wb,in}+\left[\frac{T_{w,in}+T_{wc,out}}{2}+\left(T_e-T_{wb,in}\right)e^{-NTU}\right] \tag{7}$$

where: $T_{wc,out}$ was the air temperature at the outlet of the wet curtain, ℃; $T_{wb,in}$ was the temperature of the water in the wet curtain, ℃; T_e was the environment temperature, ℃; *NTU* was the number of heat transfer units.

The number of heat transfer units (NTU) was defined as (*Bergman et al., 2011*):

$$NTU=\frac{A_{total}}{\dot{m}_a C_{p,eff}}\frac{k_{da}}{I}\left[0.1\left(\frac{I}{b}\right)^{0.12}\left(\frac{u_a I}{\nu_a}\right)^{0.8}Pr^{0.33}\right] \tag{8}$$

where: I was the specific surface area of the wet curtain, m^2/m^3; b was the thickness of the wet curtain, m; u_a was the velocity at which air passes through the wet curtain, m/s; Pr was Prandtl number; v_{da} was the kinematic viscosity of air, m^2/s.

The parameters employed in the mathematical model and boundary conditions were summarized in Table 2.

Table 2

Parameters of boundary conditions

Time	Environment temperature/℃	External radiation temperature/℃	Solar radiation/ W/m^2
8:00:00	27.00	13.83	522.90
9:00:00	29.00	16.70	569.41
10:00:00	31.00	19.58	595.24
11:00:00	32.50	21.75	609.10
12:00:00	33.50	23.20	614.64
13:00:00	34.00	23.92	613.14
14:00:00	34.50	24.65	604.26
15:00:00	34.00	23.92	585.85
16:00:00	33.00	22.48	552.59
17:00:00	31.50	20.31	491.56

RESULTS AND DISCUSSION

Validation

The experimental data (*Al-Ismaili, 2009*) were employed to validate the wet curtain model. The results in **Fig. 4** indicated that the relative deviation of the temperature values model ranged from 3.96% to 5.88%. In summary, the proposed mathematical model could effectively predict the heat transfer performance wet curtain in greenhouse.

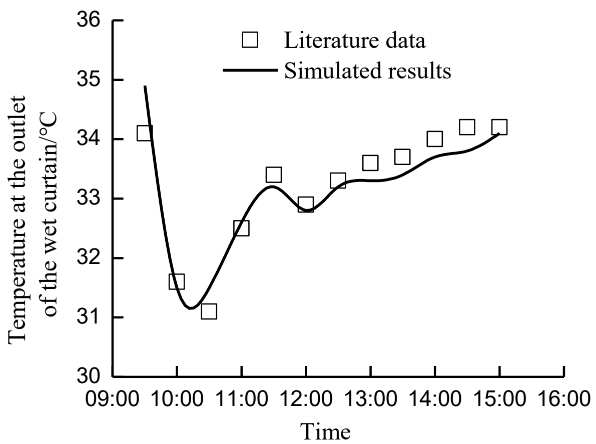

Fig. 4 - Comparison of the predicted and the measured temperature at the outlet of the wet curtain

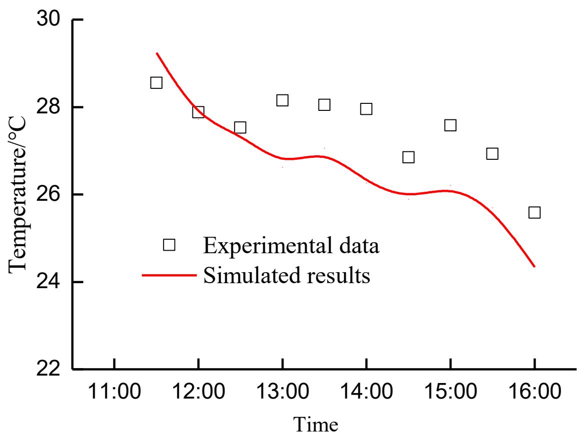

Fig. 5 - The average temperature of the greenhouse

To further substantiate the accuracy of the developed mathematical model, a comparison was conducted between the experimentally measured and numerically simulated average temperatures in the greenhouse. As illustrated in **Fig. 5**, the experimentally obtained average greenhouse temperatures were in strong agreement with the predicted results, exhibiting a relative deviation of less than 7%. The relative deviation between the experimental and simulated results might be attributed to the fact that the numerical simulation employed hourly average values of ambient temperature and solar radiation, whereas during the experimental process, these parameters exhibited fluctuations within the given hour. Based on the analyses presented in **Fig. 4** and **Fig. 5**, it could be concluded that the established mathematical model not only accurately predicted the operational performance of the wet curtain but also effectively characterized the temperature distribution within the greenhouse.

Comparison between greenhouse and wet curtain

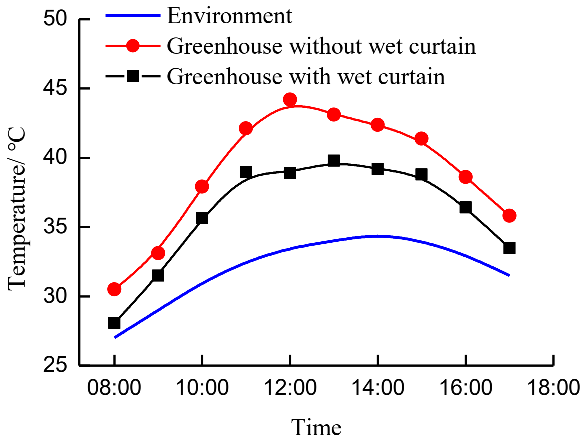

Fig. 6 - Averages temperature in greenhouse with and without wet curtain

Fig. 6 illustrated the average temperature in greenhouse with and without wet curtain on a typical day. Starting from 8:00, the initial temperatures were recorded at 30.49 °C (without wet curtain) and 28.07 °C (with wet curtain); then, given the rising ambient temperature and solar radiation, the indoor temperature progressively increased, peaking between 12:00 and 13:00 at 44.20 °C (without wet curtain) and 39.79 °C (with wet curtain); finally, temperatures gradually declining as solar radiation intensity diminished. A comparative analysis of the cooling effect of the wet curtain revealed that, during the period from 8:00 to 17:00, the wet curtain effectively reduced the ambient temperature within the greenhouse, with its cooling efficacy initially increasing and then decreasing throughout the day. At 8:00, wet curtain achieved an additional temperature reduction of 2.42 ℃ in the average greenhouse temperature, whereas at 12:00, the reduction attributable to the wet curtain reached 4.20 ℃. Subsequently, as solar radiation increased, the cooling effect of the wet curtain gradually weakened, diminishing to 2.33 °C by 17:00. The cooling capacity of the wet curtain was directly governed by its evaporation efficiency. From 8:00 to 12:00, as solar radiation intensified, the temperature difference between the outdoor air and the water in the wet curtain progressively increased, promoting the water evaporation and enhancing the actual cooling capacity of the wet curtain. After 12:00, the decrease in the solar radiation and air temperature, and the increase in the relative humidity resulted in the fact that the differences in both water vapor partial pressure and temperature between the air and the wet curtain water diminished, ultimately leading to a gradual attenuation of the cooling performance of the wet curtain.

Fig. 7 presented the temperature distribution within the greenhouse at 12:00.

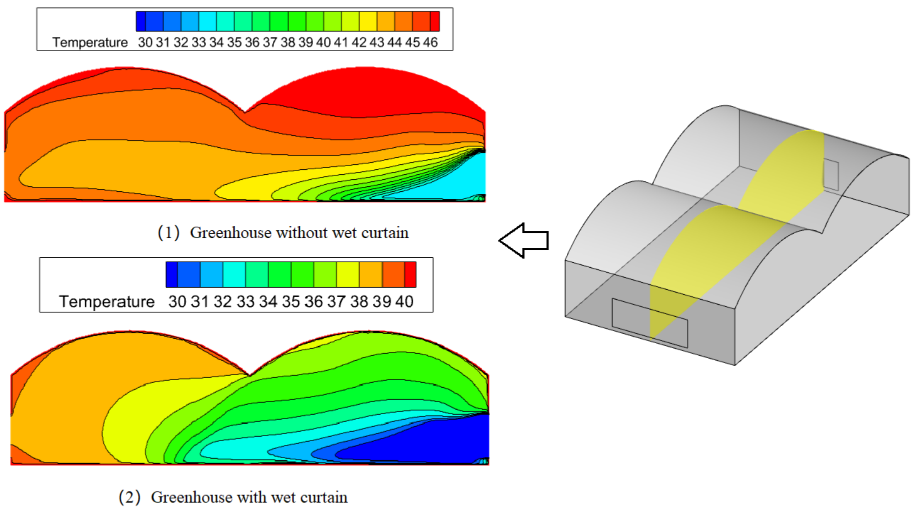

Fig. 7 - Temperature distributions in greenhouse

As illustrated in **Fig. 7**, two distinct temperature gradients appeared in the greenhouse, oriented horizontally and vertically. Owing to the transparent covering material, a substantial portion of solar radiation penetrated the greenhouse, resulting in indoor temperatures considerably higher than ambient levels.

The incoming air, either ambient or pre-cooled by the wet curtain, mixed with the warmer indoor air, thereby reducing the greenhouse temperature. The gradual intermingling of warm and cool air generated a temperature gradient along the direction of airflow. The vertical temperature gradient was influenced by two primary factors. First, because the air inlet was located at the lower portion of the greenhouse, the relatively cool air tended to accumulate near the floor under gravitational forces. Second, the polycarbonate material at the greenhouse ceiling directly absorbed a portion of the solar radiation, raising its own temperature and consequently creating a high-temperature zone near the roof.

A comparison between **Fig. 7** (1) and (2) revealed that the implementation of wet curtain substantially lowered the temperature in the crop-growing zone near the greenhouse floor. This phenomenon could be attributed to two key factors: (1) As outdoor air flowed through the wet curtain, the evaporation of water could absorb heat from the air, reducing the inlet air temperature below ambient levels. As a result, the air entering the greenhouse possessed an enhanced capacity to extract heat from the interior. (2) As depicted in **Fig. 7** (2), the cool air generated by the wet curtain gradually warmed upon entering the greenhouse. The heated air, driven by buoyancy forces, induced the natural convection beneath the greenhouse arch, as illustrated in **Fig. 9**. Such natural convection accelerates the mixing between the lower and upper regions of the greenhouse, thereby improving the uniformity of the indoor temperature distribution.

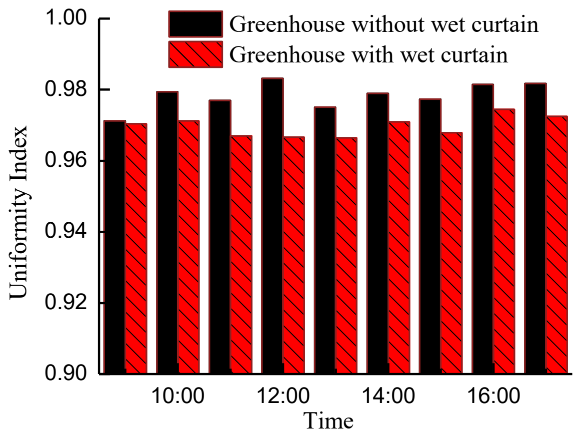

Fig. 8 - Uniformity Index of temperature with times

To better quantify the temperature distribution inside the greenhouse, **Fig. 8** presented the variation of the Uniformity Index of temperature over time.

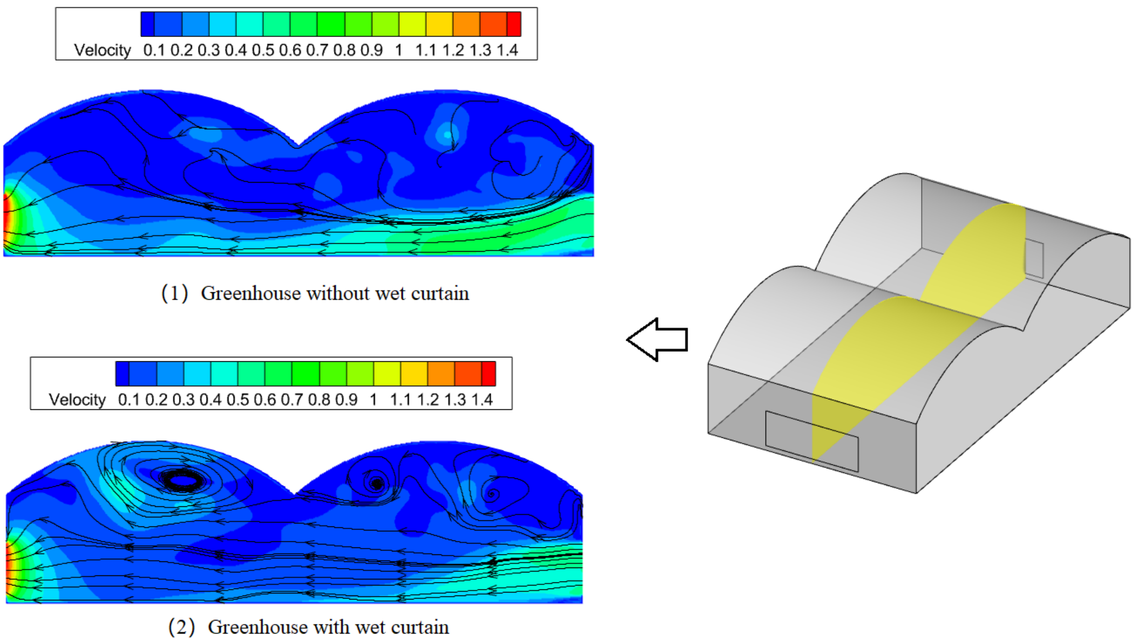

Fig. 9 - Velocity distributions in greenhouse

It could be seen from **Fig. 8**, the uniformity index under both conditions remained above 0.96 between 9:00 and 17:00, with relatively small overall fluctuations. It should be noted, however, that the uniformity index in the greenhouse without a wet curtain was slightly higher than that in the greenhouse with a wet curtain at most time points. Combined with the preceding analysis of temperature gradients, this can be explained by the fact that after the wet curtain system introduces cool air into the greenhouse, a distinct cold–hot interface forms in the horizontal airflow direction, causing a slight statistical decline in the uniformity index that measures the overall spatial distribution. Nevertheless, it is precisely this pronounced horizontal temperature difference that acts as the key driving force for the natural convection described earlier. As pointed out in the text, the cool air gradually warms after entering the greenhouse and rises under buoyancy, effectively accelerating the mixing between the cooler lower zone and the warmer upper zone of the greenhouse.

It could be found from **Fig. 9** (1) and (2) that, introducing wet curtain in greenhouse, the low-temperature air cooled by the wet curtain entered through the air inlet at a relatively high velocity, forming a stable cold air jet. This jet advanced along the ground while tending to accumulate near the greenhouse floor due to its lower temperature and higher density. As the flow developed, the cold air mixed with the warm air within the greenhouse, resulting in the decrease in its density. Under the effect of buoyancy, the warmed air gradually raised, eventually forming an updraft near the greenhouse arch. After reaching the top of the greenhouse, the ascending airflow was redirected by the enclosure. Part of the airflow moved forward and the others reversed, thereby generating two relatively regular large-scale recirculating vortices across the greenhouse cross-section. In contrast, if the greenhouse did not introduce wet curtain, the air inlet temperature was equal to the ambient temperature, resulting in a negligible density difference and weak buoyancy effects. The airflow advanced primarily in the horizontal direction, failing to establish effective vertical stratification or uplift.

Fig. 10 illustrated the temporal variation of the average air velocity in the two greenhouses. It could be seen from **Fig. 10** that from 8:00 to 12:00, the average air velocity gradually increased with times, and reached maximum values of 0.16 m/s (without wet curtain) and 0.18 m/s (with wet curtain) at 12:00, respectively. After 12:00, the average air velocity decreased. During the 8:00 ~ 12:00 period, the intensifying solar radiation raised the temperature in the greenhouse, thereby increasing the vertical temperature gradient within the greenhouse and promoting fluid mixing.

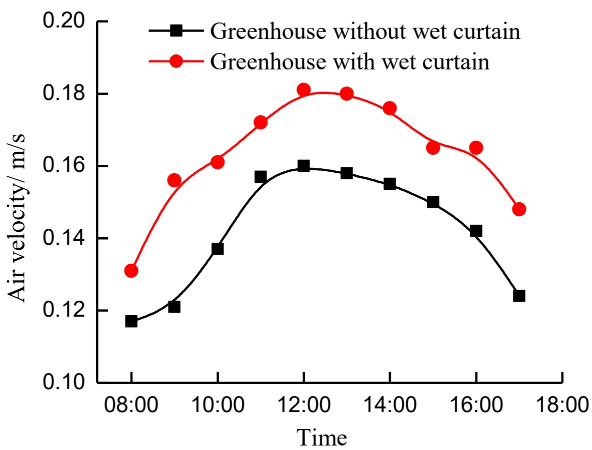

Fig. 10 - Average velocity with times

As also shown in **Fig. 10**, the implementation of pad ventilation enhances indoor air velocity, achieving an increase ranging from 8.38% to 22.40% during the 8:00 ~ 17:00 period.

The effect of the inlet velocity

Fig. 11 illustrated the average temperature in greenhouse for different inlet air velocity at 12:00. As depicted in **Fig. 11**, an increase in inlet velocity led to a gradual decline in the average greenhouse temperature, albeit with a decreasing rate of reduction. When the inlet velocity increased from 0.25 m/s to 0.5 m/s, the average greenhouse temperature decreased from 41.44 ℃ to 37.88 ℃, representing a cooling rate of 8.59%. In contrast, when the inlet velocity rose from 1.25 m/s to 1.5 m/s, the temperature reduction rate was merely 0.64%.

At low inlet velocities, the residence time of air within the wet curtain was relatively prolonged, allowing sufficient heat and moisture exchange between the air and the water in the wet curtain, thereby enabling substantial cooling. Consequently, an increase in inlet velocity effectively augmented the influx of cooled air into the greenhouse, significantly reducing the average indoor temperature.

However, as the inlet velocity continued to increase, the residence time shortened, and the heat and mass transfer between the water film and the airstream became incomplete, resulting in a diminished decline in outlet air temperature. Moreover, high inlet velocities enhanced the inertial dominance of the cold jet, causing the low-temperature air to traverse the crop zone rapidly without adequate mixing with the warm air in the greenhouse before advancing toward the outlet, thereby compromising the effectiveness of heat exchange. Hence, the reduction in average greenhouse temperature exhibited a nonlinear pattern. A comprehensive analysis of the average greenhouse temperature trends presented in **Fig. 11** indicated that once the inlet velocity exceeded 0.75 m/s, the temperature decline slowed markedly, and the marginal cooling benefit diminished. Accordingly, this study identified an inlet velocity range of 0.75 ~ 1.0 m/s as optimal for pad operation.

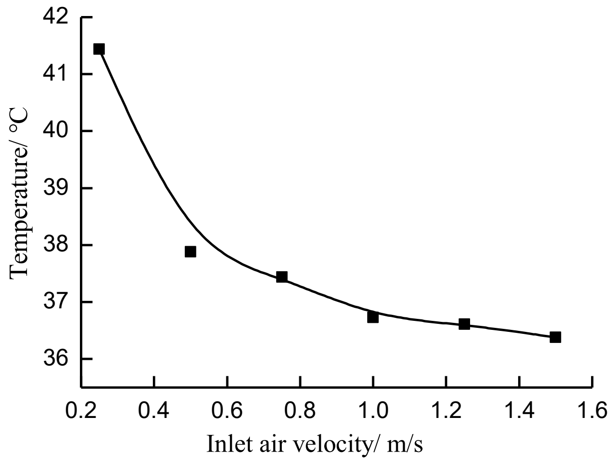

Fig. 11 - Average temperature in greenhouse for different inlet air velocity

CONCLUSIONS

A coupled numerical model of the wet curtain and greenhouse was developed and validated to investigate the mechanisms governing the influence of the wet curtain cooling system on the greenhouse thermal environment in summer. The main conclusions were as follows:

(1) The established mathematical model could accurately describe its cooling processes. The air cold by wet curtain implemented as a boundary condition for greenhouse simulations, the relative deviation between the simulated and measured average greenhouse temperatures was less than 7%, indicating that the established model effectively predicted the thermal performance of the greenhouse with wet curtain.

(2) The cooling performance of the wet curtain pronounced diurnal variation. During the period from 8:00 to 12:00, the temperature difference between the outdoor air and the water in wet curtain increased with intensifying solar radiation, enhancing the driving force for water evaporation and progressively improving cooling efficacy. After 12:00, as solar radiation weakened, the cooling capacity gradually declined. Over a typical day, the pad reduces the average greenhouse temperature by 2.33 ℃ to 4.20 ℃, with the maximum cooling effect occurring at 12:00.

(3) The cold air produced wet curtain could modify the airflow pattern within the greenhouse. Low-temperature air entered through the lower inlet as a jet, accumulated near the crop zone under gravitational forces, and subsequently rose upon heating due to buoyancy, forming two large-scale recirculating vortices across the greenhouse cross-section. This configuration effectively promoted mixing between the upper and lower air layers, resulting in a more uniform temperature distribution. Compared with forced ventilation without pad operation, the pad increased the average air velocity within the greenhouse by 8.38% to 22.40%.

(4) Parametric analysis of inlet velocity revealed that the average greenhouse temperature decreases nonlinearly with increasing inlet velocity, with the rate of reduction gradually slowing. Once the inlet velocity

exceeded 0.75 m/s, the marginal cooling benefit declined significantly. An inlet velocity in the range of 0.75 ~ 1.0 m/s was recommended.

ACKNOWLEDGMENTS

This work was supported by Doctoral Fund of Dezhou University (NO. 4022504135).

REFERENCES

[1] Abedrabboh, O., Koç, M., & Biçer, Y. (2024). Comparative thermoeconomic assessment of renewable-driven hybrid-cooled sustainable greenhouses for subtropical regions. *Energy Conversion and Management*, Vol. 300, pp.117990, Qatar.
[2] Al-Ismaili, A. M. (2009). Modeling of a humidification-dehumidification greenhouse in Oman [Doctoral dissertation, Cranfield University], United Kingdom.
[3] Allali, F. E., Fatnassi, H., Demrati, H., Molina Aiz, F. D., Gourdo, L., Errami, Y., Wifaya, A., & Aharoune, A. (2024). CFD-based optimization of Direct evaporative cooling systems for Canarian greenhouses in Semi-Arid regions. Energy & Buildings, Vol. 323(2024), pp. 114767, Morocco.
[4] Bergman, T. L., Lavine, A. S., Incropera, F. P., & DeWitt, D. P. (2011). *Introduction to heat transfer*. John Wiley & Sons, United States.
[5] Chen, L., Xu, L., & Wei, R. (2023). Energy-saving control algorithm of Venlo greenhouse skylight and wet curtain fan based on reinforcement learning with soft action mask. *Agriculture*, 13(1), 141, Shanghai, China.
[6] Chen J.R., (2015). Study of Indoor Environment Dynamic Simulation of Layer-House Based on the Model of Caged Pens of Porous Media, Master dissertation (基于笼养鸡只多孔介质模型的蛋鸡舍内环境动态模拟研究), Hebei University of Technology, China.
[7] Dietz, K. J., Zörb, C., & Geilfus, C. M. (2021). Drought and crop yield. *Plant Biology*, Vol. 23(6), pp. 881-893, Germany.
[8] Fu, Q., Li, X., Zhang, G., & Li, X. (2023). A temperature and vent opening couple model in solar greenhouses for vegetable cultivation based on dynamic solar heat load using computational fluid dynamics simulations. *Journal of Food Process Engineering*, Vol. 46(2), pp. e14240, Beijing/China.
[9] Garcia, G., Treccarichi, S., Ciccarello, L., Al Achkar, N., Arena, D., Soler, S., Prohens, J., & Branca, F. (2026). Agronomic performance of tomato rootstocks under Mediterranean greenhouse organic farming. *Agronomy*, Vol.16(5), pp. 515, Italy.
[10] He, X., Wang, J., Guo, S., Zhang, J., Wei, B., Sun, J., & Shu, S. (2018). Ventilation optimization of solar greenhouse with removable back walls based on CFD. *Computers and Electronics in Agriculture*, Vol. 149, pp. 16-25, Nanjing/China.
[11] Jerszurki, D., Saadon, T., Zhen, J., Agam, N., Tas, E., Rachmilevitch, S., & Lazarovitch, N. (2021). Vertical microclimate heterogeneity and dew formation in semi-closed and naturally ventilated tomato greenhouses. *Scientia Horticulturae*, Vol. 288, pp. 110271, Israel.
[12] Jiang, R., Li, Q., & Guo, F. (2023). Influence of outdoor environmental parameters on brackish water desalination system in greenhouse (室外环境参数对温室苦咸水淡化系统的影响). *Gas & Heat*, Vol. 43(5), pp. 28-34, Jinan/China.
[13] Jiao, N., Zhu, D., Jing, Y., Liu, M., & Liu, C. (2024). Research on determination method of greenhouse wet pad-fan operating parameters based on numerical simulation (基于数值模拟的温室湿帘—风机运行参数确定方法研究). *Journal of Chinese Agricultural Mechanization*, Vol. 45(5), pp. 79-84, Yangling, Shaanxi/China. DOI: 10.13733/j.jcam.issn.2095-5553.2024.05.012
[14] Krishna, H., Hebbar, S., Kumar, P., Sharma, S., Kumar, R., Tiwari, S., Maurya, S., Srivastava, K., Pal, G., Bahadur, A., & Behera, T. K. (2024). Navigating challenges and prospects in off-season vegetable production. *Vegetable Science*, 51, pp. 97-105 India.
[15] Lei, W., Lu, H., Qi, X., et al. (2023). Field measurement of environmental parameters in solar greenhouses and analysis of the application of passive ventilation. *Solar Energy*, Vol. 263, pp. 111851, Shandong/ China.
[16] Moreno-Teruel, M. Á., Molina-Aiz, F. D., López-Martínez, A., Marín-Membrive, P., Peña-Fernández, A., & Valera-Martínez, D.L. (2022). The influence of different cooling systems on the microclimate, photosynthetic activity and yield of a tomato crops (*Lycopersicum esculentum Mill*.) in Mediterranean greenhouses. *Agronomy*, Vol. 12(2), pp. 524, Spain.

[17] Park, S. J., Lee, I. B., Lee, S. Y., Kim, J. G., Choi, Y. B., Decano-Valentin, C., Cho, J. H., Jeong, H. H., & Yeo, U. H. (2022). Numerical analysis of ventilation efficiency of a Korean Venlo-type greenhouse with continuous roof vents. *Agriculture,* Vol.12(9), pp. 1349, Korea.

[18] Peng, Y., Ma, X., Wang, Y., Li, M., Gao, F., Zhou, K., & Aemixay, V. (2023). Energy performance assessment of photovoltaic greenhouses in summer based on coupled optical-electrical-thermal models and plant growth requirements. *Energy Conversion and Management,* Vol. 287, pp. 117086, Kunming, China.

[19] Rahman, M. S., Manjira, S., Majumder, M. K., & Rahman, S. (2021). Socio-economic determinants of off-season summer tomato cultivation. *International Journal of Vegetable Science*, Vol. 27(3), pp. 252-259, Bangladesh.

[20] Shen, L., Xue, K., Xiao, B., & Chen, Y. (2026). Simulation of Heat Flow Field in Venlo Greenhouse in South China and Optimization of Its Cooling and Dehumidification System. *Processes*, 14(9), 1331, Guangzhou, China.

[21] Yang, Y., & Liu, Y. (2024). The impact of different natural ventilation methods on the performance of desert solar greenhouses (不同自然通风方式对沙漠日光温室性能的影响). *Agriculture and Technology*, Vol. 44(10), pp. 18-23, Tarim/China. DOI: 10.19754/j.nyyjs.20240530005

[22] Yoon, J., Song, H., & Jang, E. S. (2024). Computational fluid dynamics analysis of ventilation characteristics with various design parameters in single-span greenhouses. *Energy Sources, Part A: Recovery, Utilization, and Environmental Effects*, Vol. 46(1), pp. 11938-11951, Korea.

[23] Zhang, J., Zhao, S., Dai, A., et al. (2022). Greenhouse natural ventilation models: How do we develop with Chinese greenhouses? *Agronomy*, Vol.12(9), pp. 1995, Beijing/China.

[24] Zhang, J., Zhao, S., Dai, A., Wang, P., Liu, Z., Liang, B., & Ding, T. (2025). Microclimate prediction of solar greenhouse with pad-fan cooling systems using a machine and deep learning approach. *Agriculture*, Vol.15(20), pp. 2107, Dalian/China.

[25] Zhang, Y., Sun, W., Jin, L., Yang, H., Wang, J., & Shu, S. (2025). Computational Fluid Dynamics-Based Simulation of Ventilation in a Zigzag Plastic Greenhouse. *Horticulturae*,11(2), 175, Nanjing, China